Capacity and BER Performance Considerations on Single-carrier Frequency-domain Equalization

Fumiyuki ADACHI† Tatsunori OBARA‡ and Tetsuya Yamamoto‡
Dept. of Electrical and Communication Engineering, Graduate School of Engineering, Tohoku University
6-6-05 Aza-Aoba, Aramaki, Aoba-ku, Sendai, 980-8579 Japan
E-mail: †adachi@ecei.tohoku.ac.jp ‡{obara, yamamoto}@mobile.ecei.tohoku.ac.jp.

***Abstract*—Single-carrier (SC) waveform has a lower peak-to-average power ratio than multi-carrier waveform. Furthermore, it can exploit the channel frequency-selectivity through frequency-domain equalization (FDE) to improve the transmission performance. SC-FDE is a block transmission. The cyclic prefix (CP) is inserted in front of each data block. Instead of CP insertion, the known training sequence (TS) insertion and zero padding (ZP) can be used. In this paper, performance comparison is made among CP-, TS-, and ZP-SC in terms of the channel capacity and average bit error rate (BER) performance in a frequency-selective Rayleigh fading channel.**

Keywords-component; single-carrier, frequency-domain equalization

I. INTRODUCTION

The transfer function of broadband channel varies over the signal bandwidth (such a channel is called the frequency-selective channel) [1]. The transmitted signal spectrum is severely distorted and severe inter-symbol interference (ISI) is produced. Some advanced equalization techniques must be introduced. To avoid problems arising from the severe ISI, orthogonal frequency division multiplexing (OFDM) has been attracting much attention. OFDM is a block transmission using a number of orthogonal subcarriers. Before the transmission, the cyclic prefix (CP) is inserted in front of each OFDM signal to make the received OFDM signal to be a circular convolution of the transmitted OFDM signal and the channel impulse response. Each data symbol in a block is transmitted in parallel using a different orthogonal subcarrier and hence, simple one-tap frequency-domain equalization (i.e., zero-forcing FDE) can be used [2]. However, the OFDM waveform has a high peak-to-average power ratio (PAPR) and furthermore, cannot exploit the channel frequency-selectivity.

Recently, the single-carrier with frequency-domain equalization (SC-FDE) has been gaining popularity [3]. The SC waveform has an advantage of lower PAPR than the OFDM waveform. In SC transmissions, each data symbol in a block is spread over the entire subcarriers unlike OFDM. Therefore, the use of FDE can exploit the channel frequency-selectivity to improve the transmission performance. Instead of CP insertion, the known training sequence (TS) insertion [4] and zero padding (ZP) [5] can be used.

To the best of authors' knowledge, no literature is available which gives the performance comparison among three SC-FDE schemes. In this paper, the performance comparison is made among CP-, TS-, and ZP-SC in terms of the achievable channel capacity and average bit error rate (BER) performance under the same channel condition.

The remainder of this paper is organized as follows. Section II reviews CP-, TS-, and ZP-SC. In Section III, the channel capacity expression is presented. Section IV presents the frequency-domain block signal detection. Section V discusses the channel capacity and BER performance. Section VI offers some concluding remarks.

II. CP-, TS-, AND ZP-SC

A SC block transmission of N_c data symbols is considered. Transmitter/receiver structure is illustrated for CP-, TS-, and ZP-SC in Fig. 1. If a CP of length longer than the channel maximum time delay is inserted, the received signal is a circular convolution of the transmitted block and the channel impulse response. Figure 2 illustrates the transmit data block and time-domain channel matrix. The channel maximum time delay is assumed to be N_g symbols. For CP-SC, the CP is the last N_g-symbol part in an N_c-symbol data block. For TS- and ZP-SC, the same N_g-symbol training sequence and N_g-zero sequence are respectively inserted in front of each N_c-symbol data block. They can be viewed as a CP of an N_c+N_g-symbol block.

The received signal can be expressed using the matrix form as

$$\mathbf{y}=\begin{cases}\sqrt{2P}\mathbf{h}_{N_c}\mathbf{d}+\mathbf{n}_{N_c} & \text{for CP-SC}\\ \sqrt{2P}\mathbf{h}_{N_c+N_g}\begin{pmatrix}\mathbf{d}\\ \mathbf{q}\end{pmatrix}+\mathbf{n}_{N_c+N_g} & \text{for TS-SC}\\ \sqrt{2P\cdot(1+N_g/N_c)}\mathbf{h}_{N_c+N_g}\begin{pmatrix}\mathbf{d}\\ \mathbf{0}\end{pmatrix}+\mathbf{n}_{N_c+N_g} & \text{for ZP-SC}\end{cases}, \quad (1)$$

where $\mathbf{d}$, $\mathbf{h}$, and $\mathbf{n}$ represent a transmitted data block of size N_c, the circulant time-domain channel matrix, and the noise, respectively. The size of matrix $\mathbf{h}$ is $N_c\times N_c$ for CP-SC and $(N_c+N_g)\times(N_c+N_g)$ for TS- and ZP-SC. $\mathbf{q}$ and $\mathbf{0}$ are a TS of N_g symbols and a column vector of N_g zero's, respectively. The size of $\mathbf{n}$ is N_c for CP-SC and N_c+N_g for TS- and ZP-SC. P denotes the average transmit power. In the case of ZP-SC, the signal power in the N_c-data symbol interval can be increased by a factor of $1+N_g/N_c$.

978-1-4577-0031-6/11/$26.00 ©2011 IEEE

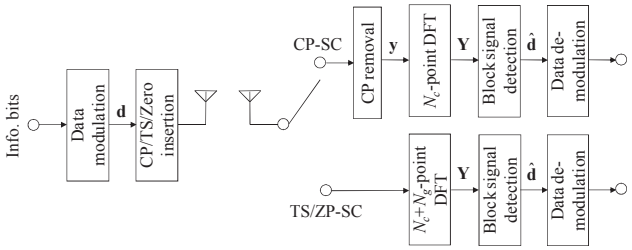

Figure 1. Transmitter/receiver structure.

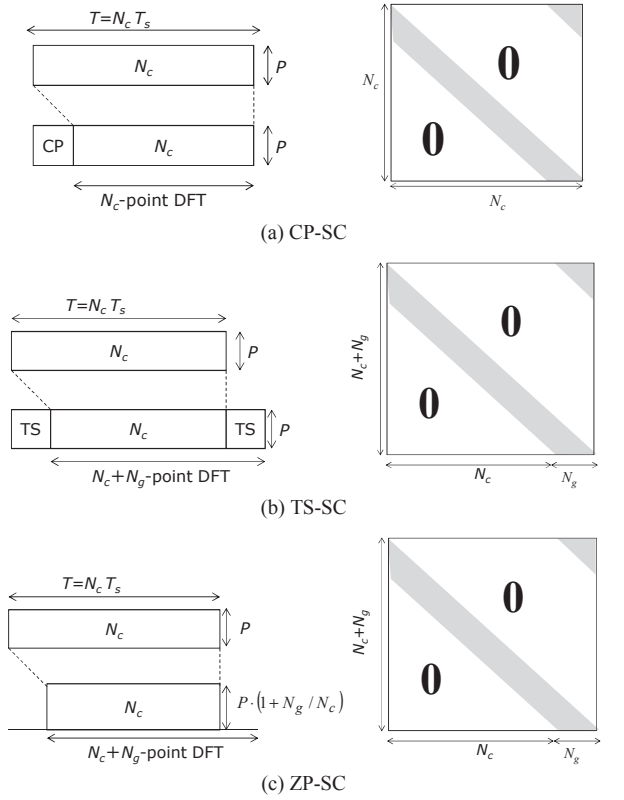

Figure 2. Transmit block and time-domain channel matrix.

III. Channel Capacity

The insertion of CP, TS, or ZP of length N_g symbols expands the signal bandwidth by a factor of $1+N_g/N_c$. The channel capacity C (bps/Hz) is expressed as [6]

$$C=\begin{cases}\dfrac{1}{1+N_g/N_c}\dfrac{1}{N_c}\log_2\det\left(\mathbf{I}+\dfrac{E_s/N_0}{1+N_g/N_c}\mathbf{h}_{N_c}\mathbf{h}_{N_c}^H\right) & \text{for CP-SC}\\ \dfrac{1}{1+N_g/N_c}\dfrac{1}{N_c}\log_2\det\left(\mathbf{I}+\dfrac{E_s}{N_0}\tilde{\mathbf{h}}_{N_c+N_g}^H\tilde{\mathbf{h}}_{N_c+N_g}\right) & \text{for TS/ ZP-SC}\end{cases}, \quad (2)$$

where $\mathbf{I}$ is the identity matrix and $\tilde{\mathbf{h}}_{N_c+N_g}$ is a matrix of size $(N_c+N_g)\times N_c$ whose N_c columns are taken from the $0\sim N_c-1$th columns of $\mathbf{h}_{N_c+N_g}$.

A. CP-SC

Since $\mathbf{h}_{N_c}$ is a circulant matrix of size $N_c\times N_c$, $\mathbf{h}_{N_c}=\mathbf{F}^H\mathbf{H}_{N_c}\mathbf{F}$ and $\mathbf{H}_{N_c}=diag\{H_{N_c}(k);k=0\sim N_c-1\}$, where $\mathbf{F}$ is the discrete Fourier transform (DFT) matrix of size $N_c\times N_c$. Hence, we have

$$\mathbf{I}+\frac{E_s/N_0}{1+N_g/N_c}\mathbf{h}_{N_c}\mathbf{h}_{N_c}^H=\mathbf{F}^H\left(\mathbf{I}+\frac{E_s/N_0}{1+N_g/N_c}\mathbf{H}_{N_c}\mathbf{H}_{N_c}^H\right)\mathbf{F}. \quad (3)$$

Since [7]

$$\begin{cases}\det(\mathbf{ABC})=\det(\mathbf{A})\det(\mathbf{B})\det(\mathbf{C})\\ \det\mathbf{F}=\det\mathbf{F}^H=\mathbf{I}\end{cases}, \quad (4)$$

the channel capacity expression becomes

$$C=\frac{1}{1+N_g/N_c}\frac{1}{N_c}\sum_{k=0}^{N_c-1}\log_2\left(1+\frac{E_s/N_0}{1+N_g/N_c}\left|H_{N_c}(k)\right|^2\right). \quad (5)$$

Applying Jensen's inequality $\left(\prod_{m=0}^{M-1}x_m\right)^{1/M}\le\frac{1}{M}\sum_{m=0}^{M-1}x_m$ [8], the channel capacity can be upper-bounded as

$$C\le\frac{1}{1+N_g/N_c}\log_2\left(1+\frac{E_s/N_0}{1+N_g/N_c}\frac{1}{N_c}\sum_{k=0}^{N_c-1}\left|H_{N_c}(k)\right|^2\right). \quad (6)$$

From the Parseval's theorem,

$$\frac{1}{N_c}\sum_{k=0}^{N_c-1}\left|H_{N_c}(k)\right|^2=\sum_{\tau=0}^{N_c-1}\left|h(\tau)\right|^2, \quad (7)$$

where $\{h(\tau);\ \tau=0,1,\ldots,N_c-1\}$ is the channel impulse response. Eq. (6) can be rewritten as

$$C\le\frac{1}{1+N_g/N_c}\log_2\left(1+\frac{E_s/N_0}{1+N_g/N_c}\sum_{\tau=0}^{N_c-1}\left|h(\tau)\right|^2\right). \quad (8)$$

B. TS- SC

Applying the eigenvalue decomposition [7] to $\tilde{\mathbf{h}}_{N_c+N_g}^H\tilde{\mathbf{h}}_{N_c+N_g}$,

$$\begin{aligned}&\mathbf{I}+\frac{E_s/N_0}{1+N_g/N_c}\tilde{\mathbf{h}}_{N_c+N_g}^H\tilde{\mathbf{h}}_{N_c+N_g}\\ &=\mathbf{U}\mathbf{U}^H+\frac{E_s/N_0}{1+N_g/N_c}\mathbf{U}\mathbf{\Lambda}\mathbf{U}^H=\mathbf{U}\left(\mathbf{I}+\frac{E_s/N_0}{1+N_g/N_c}\mathbf{\Lambda}\right)\mathbf{U}^H\end{aligned}, \quad (9)$$

where $\mathbf{U}$ and $\mathbf{\Lambda}$ are respectively the unitary matrix and the diagonal matrix having eigenvalues $\{\lambda(k);\ k=0\sim N_c-1\}$ as its diagonal elements. The channel capacity expression can be given as

$$C=\frac{1}{N_c+N_g}\sum_{k=0}^{N_c-1}\log_2\left(1+\frac{E_s/N_0}{1+N_g/N_c}\lambda(k)\right). \quad (10)$$

Applying the Jensen's inequality and using $\sum_{k=0}^{N_c-1}\lambda(k)=tr\left(\tilde{\mathbf{h}}_{N_c+N_g}^H\tilde{\mathbf{h}}_{N_c+N_g}\right)$ with $tr(\mathbf{X})$ representing the trace of matrix $\mathbf{X}$ [9], the channel capacity can be upper-bounded as

$$C \le \frac{1}{1+N_g/N_c}\log_2\left(1+\frac{E_s/N_0}{1+N_g/N_c}\frac{1}{N_c}\sum_{k=0}^{N_c-1}\lambda(k)\right) = \frac{1}{1+N_g/N_c}\log_2\left(1+\frac{E_s/N_0}{1+N_g/N_c}\sum_{\tau=0}^{N_c-1}|h(\tau)|^2\right), \quad (11)$$

which is identical to CP-SC.

C. ZP-SC

Similar to TS-SC, we can show that the channel capacity of ZP-SC is upper-bounded as

$$C \le \frac{1}{1+N_g/N_c}\log_2\left(1+\frac{E_s}{N_0}\sum_{\tau=0}^{N_c-1}|h(\tau)|^2\right). \quad (12)$$

ZP-SC achieves the same capacity as CP- and TS-SC with less E_s/N_0 by a factor of $1+N_g/N_c$.

D. Distribution of Capacity Upper-bound

The channel capacity is a function of the instantaneous channel impulse response $\{h(\tau);\ \tau=0\sim N_c-1\}$ (note that $h(\tau)=0$ for $\tau=N_g\sim N_c-1$). Letting

$$\Gamma = \begin{cases} \dfrac{E_s/N_0}{1+N_g/N_c} & \text{for CP/TS-SC} \\ E_s/N_0 & \text{for ZP-SC} \end{cases} \text{ and } x = \sum_{\tau=0}^{N_c-1}|h(\tau)|^2, \quad (13)$$

we have $C \le (1+N_g/N_c)^{-1}\log_2(1+x\Gamma)$. Assuming a Rayleigh fading channel having an L-path uniform power delay profile (i.e., $E[|h(\tau)|^2]=1/L$), the probability density function (pdf) of x is given as

$$p(x) = \frac{L^L}{(L-1)!}x^{L-1}\exp(-xL). \quad (14)$$

The pdf of the capacity upper-bound is given as

$$p(C) = \frac{L^L}{(L-1)!}\frac{a\ln 2}{\Gamma^L}2^{aC}\left(2^{aC}-1\right)^{L-1}\exp\left(-\frac{L}{\Gamma}\left(2^{aC}-1\right)\right) \quad (15)$$

with $a=1+N_g/N_c$ for CP-SC. In the similar way, the pdf of the capacity upper-bound can be obtained for TS- and ZP-SC.

IV. Frequency-domain Block Signal Detection

Since TS and ZP perform as a CP by extending the DFT block size to include TS and ZP, respectively. The size of DFT matrix for TS- and ZP-SC is N_c+N_g symbols and is longer than that for CP-SC. The frequency-domain representation $\mathbf{Y}$ of the received signal is $\mathbf{Y}=\mathbf{Fy}$, where $\mathbf{F}$ is the DFT matrix, the size of which is $N_c\times N_c$ for CP-SC and $(N_c+N_g)\times(N_c+N_g)$ for TS- and ZP-SC. The k-th element of $\mathbf{Y}$ is given as

$$Y(k) = \begin{cases} \sqrt{2P}H_{N_c}(k)D(k)+N_{N_c}(k),\ k=0\sim N_c-1 \\ \qquad\qquad \text{for CP-SC} \\ \sqrt{2P}H_{N_c+N_g}(k)D_{ts}(k)+N_{N_c+N_g}(k), \\ \quad k=0\sim N_c+N_g-1 \qquad \text{for TS-SC} \\ \sqrt{2P\cdot(1+N_g/N_c)}H_{N_c+N_g}(k)D_{zp}(k) \\ +N_{N_c+N_g}(k),\ k=0\sim N_c+N_g-1 \text{ for ZP-SC} \end{cases}, \quad (16)$$

where $H_{N_c}(k)$ and $H_{N_c+N_g}(k)$ are the kth diagonal elements of $\mathbf{H}_{N_c}=\mathbf{F}\mathbf{h}_{N_c}\mathbf{F}^H$ and $\mathbf{H}_{N_c+N_c}=\mathbf{F}\mathbf{h}_{N_c+N_c}\mathbf{F}^H$, respectively.

A. FDE Based on Minimum Mean Square Error Criterion (MMSE-FDE)

MMSE-FDE is carried out on $\mathbf{Y}$, followed by inverse DFT (IDFT) to obtain the soft decision output $\hat{\mathbf{d}}$ as

$$\hat{\mathbf{d}} = \mathbf{F}^H\mathbf{W}\mathbf{Y}, \quad (17)$$

where $\mathbf{W}=diag\{W(k);\ k=0\sim N_c-1\}$ for CP-SC and $diag\{W(k);\ k=0\sim N_c+N_g-1\}$ for TS- and ZP-SC is the FDE weight matrix. The MMSE-FDE weight is the solution to minimize $e(k)=E\left[\left|d(k)-\hat{d}(k)\right|^2\right]$ and is given as

$$W(k) = \begin{cases} \dfrac{H_{N_c}^*(k)}{\frac{E_s}{N_0}\left|H_{N_c}(k)\right|^2+\left(1+N_g/N_c\right)},\ k=0\sim N_c-1 \\ \qquad\qquad \text{for CP-SC} \\ \dfrac{H_{N_c+N_g}^*(k)}{\frac{E_s}{N_0}\left|H_{N_c+N_g}(k)\right|^2+\left(1+N_g/N_c\right)}, \\ k=0\sim N_c+N_g-1 \qquad \text{for TS/ZP-SC} \end{cases}. \quad (18)$$

The IDFT output $\{\hat{d}(n);\ n=0\sim N_c-1\}$ after MMSE-FDE is the sum of the scaled version of desired symbol, the residual ISI, and the noise and is given by

$$\hat{d}(n) = \sqrt{2P}A\cdot d(n)+\text{residual ISI}+\text{noise}. \quad (19)$$

The factor A is the equivalent channel gain and is given as

$$A = \begin{cases} \dfrac{1}{N_c}\sum_{k=0}^{N_c-1}\dfrac{\left|H_{N_c}(k)\right|^2}{\frac{E_s}{N_0}\left|H_{N_c}(k)\right|^2+\left(1+N_g/N_c\right)} \text{ for CP-SC} \\ \dfrac{1}{N_c+N_g}\sum_{k=0}^{N_c+N_g-1}\dfrac{\left|H_{N_c+N_g}(k)\right|^2}{\frac{E_s}{N_0}\left|H_{N_c+N_g}(k)\right|^2+\left(1+N_g/N_c\right)} \\ \qquad\qquad \text{for TS/ZP-SC} \end{cases}. \quad (20)$$

When the channel drops (i.e., $(E_s/N_0)\left|H_{N_c}(k)\right|$ and $(E_s/N_0)\left|H_{N_c+N_c}(k)\right| << 1+N_g/N_c$), the equivalent channel gain can be approximated as

$$A \approx \begin{cases} \dfrac{1}{N_c}\sum_{k=0}^{N_c-1}\left|H_{N_c}(k)\right|^2 = \sum_{\tau=0}^{N_c-1}|h(\tau)|^2 \text{ for CP-SC} \\ \dfrac{1}{N_c+N_g}\sum_{k=0}^{N_c+N_g-1}\left|H_{N_c+N_g}(k)\right|^2 = \sum_{\tau=0}^{N_c+N_g-1}|h(\tau)|^2 \\ \qquad\qquad \text{for TS/ZP-SC} \end{cases}. \quad (21)$$

Since the channel length is shorter than the guard interval of N_g symbols, $\sum_{\tau=0}^{N_c-1}|h(\tau)|^2 = \sum_{\tau=0}^{N_c+N_g-1}|h(\tau)|^2 = \sum_{\tau=0}^{N_g-1}|h(\tau)|^2$ and hence, all of CP-, TS-, and ZP-SC achieve the same frequency-diversity order.

The soft-decision symbol block is $\{\hat{d}(n); n = 0 \sim N_c - 1\}$. In the case of TS- and ZP-SC, $\{\hat{d}(n); n = N_c \sim N_c + N_g - 1\}$ can be used for the quality measurement since the N_g-symbol part in an N_c+N_g-symbol block is known to the receiver.

B. *Frequency-domain QRM-MLBD*

A big performance gap from the matched filter-bound (MF) still exists due to the presence of residual ISI after MMSE-FDE. The maximum likelihood (ML) block detection using frequency-domain QR decomposition and M-algorithm (QRM-MLBD) [10] is a powerful signal detection combined with FDE to narrow the performance gap. The receiver structure of frequency-domain QRM-MLBD is illustrated in Fig. 3.

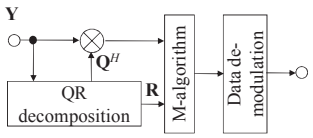

Figure 3. Frequency-domain QRM-MLBD.

Using Eq. (1), the frequency-domain signal **Y**=**Fy** is expressed as

$$\mathbf{Y} = \begin{cases} \sqrt{2P}\overline{\mathbf{H}}_{N_c}\mathbf{d} + \mathbf{N}_{N_c} & \text{for CP-SC} \\ \sqrt{2P}\overline{\mathbf{H}}_{N_c+N_g}\begin{pmatrix}\mathbf{d}\\ \mathbf{q}\end{pmatrix} + \mathbf{N}_{N_c+N_g} & \text{for TS-SC} \\ \sqrt{2P\cdot(1+N_g/N_c)}\overline{\mathbf{H}}_{N_c+N_g}\begin{pmatrix}\mathbf{d}\\ \mathbf{0}\end{pmatrix} + \mathbf{N}_{N_c+N_g} & \text{for ZP-SC} \end{cases}, \quad (22)$$

where $\overline{\mathbf{H}} = \mathbf{HF}$ is the equivalent channel matrix, the size of which is $N_c \times N_c$ for CP-SC and $(N_c+N_g)\times(N_c+N_g)$ for TS- and ZP-SC. **N** is the frequency-domain noise vector.

QRM-MLBD consists of two steps. First, the QR decomposition is applied to $\overline{\mathbf{H}}$ to obtain $\overline{\mathbf{H}} = \mathbf{QR}$, where **Q** is an unitary matrix and **R** is an upper triangular matrix. The size of **Q** and **R** is $N_c \times N_c$ for CP-SC and is $(N_c+N_g)\times(N_c+N_g)$ for TS- and ZP-SC. The transformed frequency-domain received signal is obtained as

$$\hat{\mathbf{Y}} = \mathbf{Q}^H\mathbf{Y} = \begin{cases} \sqrt{2P}\mathbf{R}\mathbf{d} + \mathbf{Q}^H\mathbf{N}_{N_c} & \text{for CP-SC} \\ \sqrt{2P}\mathbf{R}\begin{pmatrix}\mathbf{d}\\ \mathbf{q}\end{pmatrix} + \mathbf{Q}^H\mathbf{N}_{N_c+N_g} & \text{for TS-SC} \\ \sqrt{2P\cdot(1+N_g/N_c)}\mathbf{R}\begin{pmatrix}\mathbf{d}\\ \mathbf{0}\end{pmatrix} + \mathbf{Q}^H\mathbf{N}_{N_c+N_g} & \text{for TS-SC} \end{cases}. \quad (23)$$

Since **R** is the upper triangular matrix, the ML detection can be converted to the successive tree search problem and the computational complexity can be reduced by introducing the M-algorithm.

V. Performance Evaluation

The channel capacity and BER performance achievable with CP-, TS-, and ZP-SC are evaluated by numerical computation and computer simulation, respectively. Transmission/channel condition is shown in Table I. The channel is assumed to be a block Rayleigh fading channel having an L=16-path exponential power delay profile with decay factor β.

TABLE I. Transmission/ Channel Condition

Transmission	Data modulation	QPSK
	Data block size	N_c=64
	CP/TS/ZP size	N_g=16
	Equalization	MMSE-FDE, QRM-MLBD
	Channel estimation	Ideal
Channel	Fading type	L=16-path block Rayleigh
	Power delay profile	Exponential, decay factor β
	Time delay	$\tau_l = l$, l=0~L−1

A. *Channel Capacity*

Figure 4 compares the pdfs of the channel capacity upper-bound of CP-, TS-, and ZP-SC for the uniform power delay profile (the decay factor β=0dB). ZP-SC has a slightly higher capacity than CP- and TS-SC since the signal-to-noise power ratio (SNR) is increased by a factor of $1+N_g/N_c$ for the given average signal power P. The channel capacity varies according to the changes in the instantaneous channel impulse response shape when a mobile terminal moves.

Figure 5 plots the average capacity as a function of E_s/N_0 with β as a parameter. As β increases, the average capacity reduces due to the less frequency diversity (path diversity) gain.

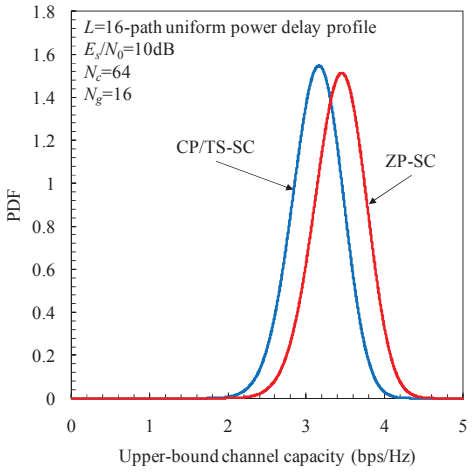

Figure 4. Pdf of channel capacity upper-bound.

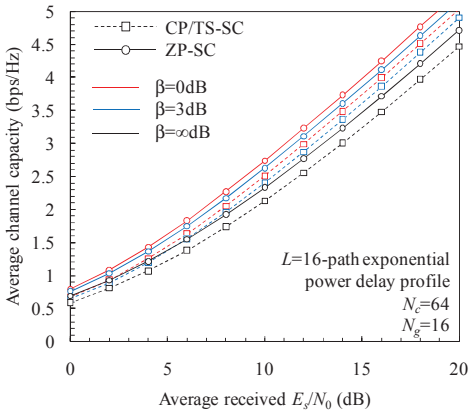

Figure 5. Average channel capacity.

B. BER Performance

Figure 6 plots the BER performance of MMSE-FDE as a function of average received bit energy-to-noise power spectrum density ratio E_b/N_0 (=$(E_s/N_0)/2$). The MF bound [11] is also plotted. CP- and TS-SC achieve the identical BER performance. ZP-SC is the best among three SC schemes. However, still a big performance gap from the MF bound exists.

Figure 7 compares the BER performances achievable with QRM-MLBD and MMSE-FDE assuming the uniform power delay profile (β=0dB). For QRM-MLBD, M=4, 16, and 64 are considered. Also plotted is the MF bound. QRM-MLBD outperforms MMSE-FDE. It provides better performance and approaches the MF bound by increasing the number M of surviving paths in the M-algorithm. It should be noted that increasing M increases the computational complexity. ZP-SC provides the best BER performance close to the MF bound even using M=8.

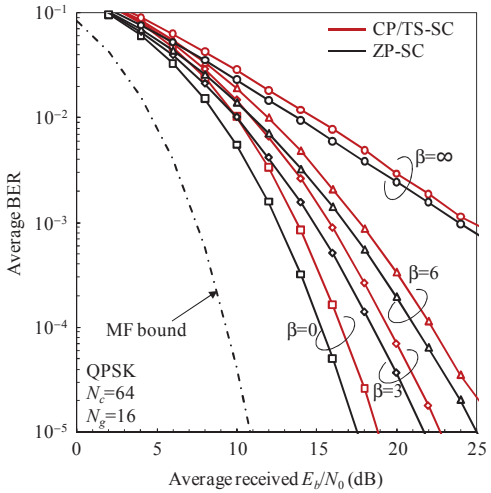

Figure 6. BER performance of MMSE-FDE.

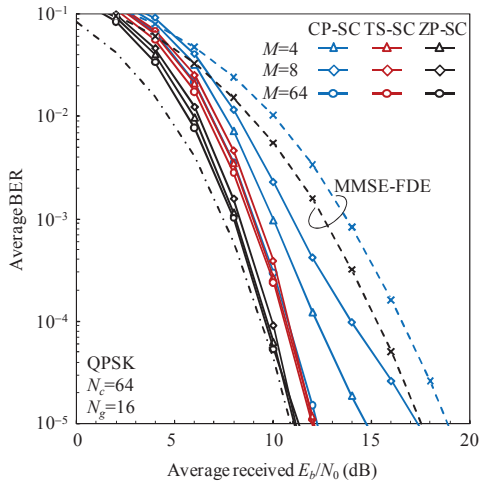

Figure 7. BER performance comparison.

VI. Conclusion

In this paper, we discussed the channel capacity and BER performance achievable with CP-, TS-, and ZP-SC. It was shown that ZP-SC is the best among three SC schemes. Although ZP-SC is the best, TS-SC remains as a promising transmission scheme. In TS-SC, the known TS is transmitted every data block and can be used for channel estimation. TS-SC channel estimation is very robust against fast fading.

References

[1] W. C. Jakes, Jr., ed., *Microwave Mobile Communications*, John Wiley & Sons, Newyork, 1974.

[2] S. Hara and R. Rasad, "Overview of multicarrier CDMA," IEEE Commun. Mag., Vol. 35, No. 12, pp. 126-133, Dec. 1997.

[3] D. Falconer, S. L. Ariyavisitakul, A. Benyamin-Seeyar, and B. Edison, "Frequency domain equalization for single-carrier broadband wireless systems," IEEE Commun. Mag., Vol. 40, No. 4, pp. 58-66. Apr. 2002.

[4] L. Deneire, B. Gyselinckx, and M. Engels, "Training sequence versus cyclic prefix - a new look on single carrier communication," IEEE Commun. Lett., Vol. 5, No. 7, pp. 292-294, Jul. 2001.

[5] A. Scaglione, G. B. Giannakis, and S. Barbarossa, "Redundant filter bank precoders and equalizers -Part I: Unification and optimal designs and Part II: Blind-channel estimation, synchronization, and direct equalization," IEEE Trans. Signal Process., Vol. 47, No. 7, pp. 1988-2022, Jul. 1999.

[6] B. Holter, "On the capacity of the MIMO channel - A tutorial introduction," Proc. Norwegian Signal Processing Conference, Trondheim, Norway, Oct. 2001.

[7] G. H. Golub and C. F. van Loan, *Matrix Computations*, 3rd ed. Baltimore, MD, Johns Hopkins Univ. Press, 1996.

[8] I.S.Gradshteyn and I.M.Ryzhik, *Table of integrals, series, and products*,New York, Academic Press, 1965.

[9] G. A. Korn and T.M.Korn, *Mathematical handbook for scientists and engineers*, Dover Publications,2000.

[10] T. Yamamoto, K. Takeda, and F. Adachi, "Frequency-domain block signal detection with QRM-MLD for training sequence-aided single-carrier transmission," EURASIP Journal on Advances in Signal Processing, Vol. 2011, Article ID 575706, 12 pages, 2010. doi: 10.1155/2011/575706.

[11] F. Adachi and K. Takeda, "Bit error rate analysis of DS-CDMA with joint frequency-domain equalization and antenna diversity combining," IEICE Trans. Commun., Vol. E87-B, No. 10, pp.2991-3002, Oct. 2004.